Fluid Phase Equilibria 586 (2024) 114193

Contents lists available at ScienceDirect

Fluid Phase Equilibria

journal homepage: www.journals.elsevier.com/fluid phase equilibria

Novel Green Aqueous Two-Phase Systems (ATPSs) based on choline salts and application to the removal of pharmaceutical pollutants from water

Leonor R. Barroca [a,b], Pedro Velho [a,b,*], Eugenia A. Macedo [a,b,*]

[a] LSRE-LCM – Laboratory of Separation and Reaction Engineering - Laboratory of Catalysis and Materials, Faculty of Engineering, University of Porto, Rua Dr. Roberto Frias, 4200-465 Porto, Portugal

[b] ALiCE – Associate Laboratory in Chemical Engineering, Faculty of Engineering, University of Porto, Rua Dr. Roberto Frias, 4200-465 Porto, Portugal

ARTICLE INFO

Keywords:
Choline salts
Liquid-liquid equilibria
Aqueous two-phase systems
Active pharmaceutical ingredients

ABSTRACT

Aqueous Two-Phase Systems (ATPSs) constitute extractive media with applicability for the removal of a wide range of solutes, such as antioxidants or pharmaceuticals, and can be designed in a non-toxic and environmentally friendly manner. Nevertheless, prior to their general use at large scale, their liquid-liquid equilibria (solubility curves and tie-line compositions) need to be thoroughly determined.

In this work, 6 solubility curves were obtained for novel aqueous ternary systems containing choline salts (choline chloride, choline bicarbonate, choline (2R,3R)-bitartrate and choline di-hydrogen citrate) and either ethyl lactate (EL) or polyethylene glycol (PEG), at 298.15 K and 0.1 MPa. Moreover, 3 tie-line compositions were successfully determined for the system {ethyl lactate (1) + choline (2R,3R)-bitartrate (2) + water (3)}. Then, this novel ATPS was applied in the removal of three common pharmaceutical pollutants from aqueous media (acetaminophen, amoxicillin and salicylic acid). In these partition studies, salicylic acid and acetaminophen were effectively extracted to the top phase, with the highest partition coefficients ($K = 9 \pm 2$) being obtained for salicylic acid in the longest tie-line (length of 0.8816). Acetaminophen achieved the most promising results ($K = 2\,2 \pm 0\,1$) in the shortest tie-line (length of 0.6192).

1. Introduction

The widespread intake and subsequent disposal of pharmaceuticals, along with their associated packaging, have caused the contamination of both soil and water bodies by active pharmaceutical ingredients (APIs). Therefore, the development of efficient and eco-friendly approaches is vital to remove these pollutants from water and replace currently used techniques, such as adsorption, advanced oxidation processes (AOPs) and membrane processes [1].

Amongst the emerging alternatives are Aqueous Two-Phase Systems (ATPSs), also referred to as Aqueous Biphasic Systems (ABSs), which are known for the extraction of bioactive compounds [2] (*e.g.,* pigments [3,4], amino acids or proteins [5]), polyphenolic compounds [6,7], and active pharmaceutical ingredients [8-13]. ATPSs are generally composed of two phases with high water content, are efficient for a wide range of applications, especially for the concentration and purification of biomolecules [14], and are considered cost-effective.

Furthermore, ATPSs are generally ternary systems composed by two species with a considerable solubility in water, such as two polymers, two salts, a salt and a polymer, or a salt and a solvent [15]. Concerning polymers, polyethylene glycol (PEG) with various molecular masses is often used, due to its low environmental impact and high phase separation ability [16,17]. Additionally, since the 1980s, ionic liquid-based ATPSs have been studied as promising extraction media [18], with a more recent focus on green ionic liquids (ILs), including, for example, Choline-Amino Acid Ionic Liquids (CAAILs). As opposed to imidazolium- and pyridinium-based ILs, CAAILs are biodegradable, non-toxic and highly biocompatible [18,19], with past applications in liquid-liquid extractions of bioactive molecules such as amino-acid derivatives [18] or pharmaceuticals [15]. Both organic and inorganic salts have been studied so far in the literature [17,18,20-22].

Even though a notable attention has been paid to ionic liquid-based ATPSs in recent years, several studies have delved into ATPSs containing ethyl lactate (EL) [6,9,20,23,24]. EL is an environmentally friendly solvent derived from lactic acid and can be generated from biomass raw materials through fermentation [25]. Furthermore, this solvent has attracted growing attention due to its low viscosity, high biodegradability, and high non-toxicity [25].

* Corresponding authors.
E-mail addresses: velho@fe.up.pt (P. Velho), eamacedo@fe.up.pt (E.A. Macedo).

https://doi.org/10.1016/j.fluid.2024.114193
Received 9 May 2024; Received in revised form 21 July 2024; Accepted 26 July 2024
Available online 29 July 2024

More particularly, ethyl lactate-based ATPSs have been successfully applied in the extraction of polyphenols and vitamins. For instance, Kamalanathan, et al. [26] have extracted catechin and caffeine using {EL (1) + trisodium citrate or disodium tartrate or disodium succinate (2) + water (3)}. EL-based systems have also been applied in the partition of polyphenols and vitamins, such as rutin, quercetin, riboflavin, epicatechin, cyanocobalamin and nicotinic acid [6,20,21,23]. In the last year, Velho and Macedo [27] have applied the ternary system {EL (1) + sodium potassium tartrate (2) + water (3)} in the partition of epicatechin, cyanocobalamin, syringic acid, and vitamin B9, whilst several ATPSs containing EL and organic salts been used in the extraction of antioxidants such as resveratrol [28], ferulic acid, and gallic acid [7,29].

These biphasic systems have also been used with other classes of solutes, such as APIs. Zakrzewska, et al. [9] have successfully extracted antibiotics, namely chloramphenicol and tetracycline, from aqueous samples using ATPSs containing EL and inorganic salts (thiosulfate salts $Na_2S_2O_3$, $K_2S_2O_3$ and $(NH_4)_2S_2O_3$). Salicylic acid was partitioned using five different EL-based ternary systems, containing organic salts [30]. Finally, ATPSs composed of EL and inorganic salts (K_3PO_4, K_2HPO_4 and K_2CO_3) were used for the separation of amino acids (L-phenylalanine, L-tryptophan and L-tyrosine) by Kamalanathan, et al. [31].

There are several reports in literature of liquid-liquid equilibria (LLE) of ternary systems containing ethyl lactate and salts (either organic or inorganic), but few LLE reports regarding EL- or polymer-based ATPSs with choline salts were found ([32-35]). The cation in choline salts is the cholinium ion, commonly called choline (an essential micronutrient that belongs to the class of B vitamins, found in eggs, peanuts, meat and vegetables [36]), whereas the anion in these salts can be either organic (such as tartrate or citrate ions) or inorganic (such as bicarbonate or chloride ions).

This work aimed to determine the liquid-liquid equilibria of new eco-friendly ATPSs based on biocompatible phase-forming components (choline salts and either ethyl lactate or green polymers) and use them in the removal of pharmaceutical pollutants from water, at 298.15 K and 0.1 MPa, in the search for a more sustainable approach to water treatment.

2. Experimental

2.1. Chemicals

In Table 1, the list of chemicals used can be found, as well as their respective molar masses, commercial suppliers, purities, Chemical Abstracts Service (CAS) numbers and abbreviations. All chemicals used in this study were recently purchased, for which they were not further purified. Prior to experiments, the water content of hygroscopic components was confirmed to be the one provided by the suppliers using Karl-Fischer titration, and this contamination was taken into account during solution preparation.

2.2. Apparatus

In this work, mass (m) was quantified using an Adam Equipment balance model AAA250L with a standard measurement uncertainty of 1·10 ^{4} g. pH values were measured with a VWR pH 1100 L pH meter with standard measurement uncertainties of 0 01 in pH and 0 1 K in temperature. Liquid densities (ρ) were assessed using an Anton Paar DSA 4500 M densimeter, with standard measurement uncertainties of 1·10 ^{5} g·cm ^{3} and 0 01 K. Electrical conductivity was measured using a Hanna EDGE EC conductivity meter, coupled with a platinum conductivity cell HI763100, with a relative measurement uncertainty of 1 %. Temperature (T) was kept constant in a thermoregulated bath (Bath OvanTherm MultiMix BHM5E) with a standard measurement uncertainty of 0 01 K. Samples were stirred either on a VWR vortex VV3 or on an IKA RO 10P magnetic stirrer.

Moreover, the Ultraviolet-Visible (UV–Vis) absorbance spectra were determined at 298.15 K, on a Greiner bio-one polystyrene flat bottom plate with 96 wells, with the Thermo Scientific Varioskan Flash UV–Vis spectrophotometer, from 200 to 600 nm, by pipetting 200 L on the plate with an Eppendorf Multipipette E3x. UV–Vis absorbance (A) measurements had a standard measurement uncertainty of 10 ^{4}. When pipetting with the Eppendorf Multipipette E3x using the 200 L tips, volumes had a relative measurement uncertainty of 0 01.

2.3. Liquid-liquid equilibria (LLE) determination

2.3.1. Determination of solubility curves

The solubility curves of several ternary aqueous systems containing a choline salt were studied in this work. Besides water, the ternary systems also contained ethyl lactate (EL) or a green polymer, either polyethylene glycol (PEG) or polyvinylpyrrolidone (PVP).

Therefore, the cloud-point method, a visual method widely described in literature [17,20], was employed to determine the solubility curve of each system at 298.15 K and 0.1 MPa. Briefly, this method consists of titrating EL or a close to saturated polymer solution (component 1) using a close to saturated salt stock solution (component 2). First, droplets of a close to saturated salt solution (component 2) were added to a known mass of component 1 until turbidity was achieved (cloud-point). Then, droplets of ultrapure water were added until the solution became clear and homogeneous again. Composition of the cloudy and clear solutions were determined by mass quantification, obtaining the mass fractions (w_i) of all components. Finally, plotting compositions allowed to obtain the solubility curve of each system.

Table 1
List of chemicals used, with molar masses (M), chemical formula, suppliers, purities, CAS numbers and abbreviations.

Chemical	M / g·mol ^{1}	CAS	Supplier	Purity [a] /%	Abbreviation [b]
(-)-Ethyl L-lactate ($C_5H_{10}O_3$)	118.13	687–47–8	Aldrich	98	EL
Acetaminophen ($C_8H_9NO_2$)	151.16	103–90–2	Cayman Chemical Europe	98	Acet
Acetic acid (CH_3CO_2H)	60.05	64–19–7	Merck	99.8	–
Amoxicillin trihydrate ($C_{16}H_{19}N_3O_5S•3H_2O$)	419.5	61,336–70–7	Tokyo Chemical Industry	98	Amox
Choline bicarbonate, in solution (80 % in water) ($C_6H_{15}NO_4$)	165.19	78–73–9	Sigma	98	[Ch][Bic]
Choline (2R,3R)-bitartrate ($C_9H_{19}NO_7$)	253.25	87–67–2	abcr GmbH	98	[Ch][Bit]
Choline chloride ($C_5H_{14}NOCl$)	139.62	67–48–1	VWR Chemicals	99	[Ch]Cl
Choline di-hydrogen citrate ($C_{11}H_{21}NO_8$)	295.29	77–91–8	Tokyo Chemical Industry	99	[Ch][DHCit]
Polyethylene glycol 1500 ($C_{2n}H_{4n+2}O_{n+1}$)	~ 1500	25,322–68–3	Merck	–	PEG1500
Polyethylene glycol 4000 ($C_{2n}H_{4n+2}O_{n+1}$)	~ 400	25,322–68–3	Merck	–	PEG4000
Polyvinylpyrrolidone 29 000 ($C_{6n}H_{9n+2}N_nO_n$)	~ 29 000	9003–39–8	Aldrich	–	PVP29000
Salicylic acid ($C_7H_6O_3$)	138.12	69–72–7	Sigma-Aldrich	99	SA
Sodium hydroxide (NaOH)	40.00	1310–73–2	Merck	99	–
Water (H_2O)	18.02	7732–18–5	VWR Chemicals	–	–

[a] Provided by the supplier in mass percentage.
[b] In hydrates, abbreviations refer to the anhydrous components.

In literature, there are several empirical correlations reported for the description of solubility curve data, such as the Merchuk equation [37] (Eq. (1)), the Li equation [38] (Eq. (2)), and the Yu equation [39] (Eq. (3)):

$$w_1 = A_1 \cdot e^{\left(B_1\ w_2^{0\,5}\ \ C_1\ w_2^3\right)} \tag{1}$$

$$w_1 = A_1 + B_1\ w_2{}^{0\,5} + C_1\ w_2 + D_1\ w_2^2 \tag{2}$$

$$w_1 = e^{\left(A_1 + B_1\ w_2^{0\,5} + C_1\ w_2 + D_1\ w_2^2\right)} \tag{3}$$

where w_i are the mass fractions of component i, and A_1, B_1, C_1 and D_1 are adjustable parameters.

2.3.2. Determination of tie-line compositions

Following the determination of the solubility curves, the geometry (area and shape) of the obtained curves was assessed. If the area above the solubility curve (heterogeneous zone) was considered sufficient, then that system was selected for further studies.

The composition of two phases in equilibrium was determined by intersecting third-degree polynomials of two independent thermophysical properties: in this work, liquid density (ρ) and electrical conductivity ( ) were chosen. For this, binary and ternary mixtures with known composition were prepared in the homogeneous region (below the solubility curve). After being stirred in a vortex for 30 s to ensure homogeneity, liquid density and electrical conductivity were measured in triplicate. Then, the data were fitted to third-degree polynomials with respect to composition, as Eq. (4) shows.

$$Q = \sum_{i=1}^{3} \sum_{j=1}^{n_{species}} k_{ij} w_j^i \tag{4}$$

where Q stands for either liquid density (ρ) or electrical conductivity ( ), $n_{species}$ for the number of species in the system, k_{ij} for the adjustable parameters, and w_j^i for the mass fraction of component j to the power of i (which ranges from 1 to 3).

The k_{ij} parameters were obtained by minimizing the Root Mean Squared Error (RMSE), as it is common in literature and in the research group [15,40]. The degree of the polynomial was verified by performing an F-test and the validity of the fittings was evaluated by assessing two performance indicators: the RMSE and the determination coefficient R^2).

The next step was to determine tie-line compositions, for which initial mixture compositions were selected in the biphasic region and prepared in triplicate. Vials containing 10 g of the initial mixture were prepared by pipetting and measuring the mass of each compound. The vials were capped and sealed, and the initial ternary mixtures were stirred for 6 h at 298.15 K, then settled overnight (approximately 12 h) at the same temperature. This ensured that the mixtures split into a top and a bottom phase, which were separated using an Eppendorf Multipipette E3x. Mass, UV–Vis absorbance from 200 to 600 nm, pH, electrical conductivity, and liquid density of each phase were measured as described in Section 2.2.

The compositions of the top and bottom phases were determined by simultaneously minimizing the difference between the experimental (exp) and calculated (calc) physical properties (liquid density (ρ) and electrical conductivity ( ), Eqs. (5) and (6), respectively) and verifying that the sum of all mass fractions relative to the same phase (w_i) corresponded to unity (Eq. (7)).

$$\rho_{exp} \quad \rho_{calc} = 0 \tag{5}$$

$$_{exp} \quad _{calc} = 0 \tag{6}$$

$$\sum w_i \quad 1 = 0 \tag{7}$$

where w_i is the mass fraction of component i in each phase (top or bottom) or in the initial mixture, and exp and calc refer to the experimental and calculated physical properties, respectively. The calculated properties, ρ or , were determined by applying the polynomials resulting from Eq. (4).

Lastly, the tie-line length (TLL, Eq. (8)) and slope (STL, Eq. (9)) were calculated as follow:

$$\mathrm{TLL} = \sqrt{\left(w_1^{\mathrm{T}} \quad w_1^{\mathrm{B}}\right)^2 + \left(w_2^{\mathrm{T}} \quad w_2^{\mathrm{B}}\right)^2} \tag{8}$$

$$\mathrm{STL} = \frac{w_2^{\mathrm{T}} \quad w_2^{\mathrm{B}}}{w_1^{\mathrm{T}} \quad w_1^{\mathrm{B}}} \tag{9}$$

Several empirical correlations are often used to establish relations between the mass fractions of the different components, being the most widely used the ones proposed by Othmer-Tobias [41], Eq. (10), and by Bancroft-Hubard [42], Eq. (11). However, it must be noted that these equations should not be used to evaluate the "quality" nor the "reliability" of the LLE data since they have an empirical basis [43].

$$\ln\left(\frac{1 \quad w_1^{\mathrm{T}}}{w_1^{\mathrm{T}}}\right) = S_{\mathrm{OT}} + n_{\mathrm{OT}} \ln\left(\frac{1 \quad w_2^{\mathrm{B}}}{w_2^{\mathrm{B}}}\right) \tag{10}$$

$$\ln\left(\frac{w_3^{\mathrm{B}}}{w_2^{\mathrm{B}}}\right) = S_{\mathrm{BH}} + n_{\mathrm{BH}} \ln\left(\frac{w_3^{\mathrm{T}}}{w_1^{\mathrm{T}}}\right) \tag{11}$$

where S_{OT}, n_{OT}, S_{BH} and n_{BH} are adjustable parameters, w_i is the mass fraction of component i, and ln is the natural logarithm. Superscripts T and B refer to the top (rich in EL, component 1) and bottom (rich in salt, component 2) phases, respectively.

2.4. Partitions in the selected ATPS

In the liquid-liquid extractions (partitions) of the pharmaceuticals acetaminophen, amoxicillin, and salicylic acid, the methodology of recent works from the research group [7,23,44] was followed, involving: study of the effect of pH on UV–Vis absorbance; stability study of UV–Vis absorbance spectra with time; UV–Vis calibration curve determination; blank assessment and partition assays.

2.4.1. pH effect on UV–Vis absorbance

To determine the mean charge of a solute as a function of pH, the values of the negative base-10 logarithm of each acid dissociation constant (pK_a) were found in literature. Then, the ratio between two successive stages of the solute was calculated, for a given pH, using Eq. (12) [7,23,44]:

$$\frac{\left[\mathrm{S}^{q_0\ \ (i\ \ 1)}\right]}{\left[\mathrm{S}^{q_0\ \ i}\right]} = 10^{\mathrm{pH}_\varphi\ \ pK_a^i} \tag{12}$$

where S stands for the solute, q_0 is the initial electrical charge at pH $= 0$, pH_φ denotes the pH of phase φ and $\mathrm{p}K_a^i$ is the pK_a relative to the stage i. The value of i varies from 0 to the maximum number of protons the species can donate (which is the number of dissociation constants). $\left[\mathrm{S}^{q_0\ \ (i\ \ 1)}\right]$ and $\left[\mathrm{S}^{q_0\ \ i}\right]$ are the mole concentrations of the solute with electrical charges equal to $q_0 \quad (i \quad 1)$ e and $q_0 \quad i$ elementary charges (also denoted e, $1\,602{\cdot}10^{\ 19}$ C).

The mean electrical charge $\overline{q}$ of a solution can be calculated as shown in Eqs. (13) and (14) [7,23,44]. These connect the relative abundances of each charged solute stage and their respective charge.

$$\overline{q} = \sum_{i=1}^{i_{max}} \left[x_{\mathrm{S}^{q_0\ \ (i\ \ 1)}} \cdot (q_0 \quad (i \quad 1))\right] + \left[1 \quad \sum_{i=1}^{i_{max}} x_{\mathrm{S}^{q_0\ \ (i\ \ 1)}}\right] \cdot (q_0 \quad i_{max}) \tag{13}$$

$$x_{S^{q_0\ (i\ 1)}} = \frac{\left[S^{q_0\ (i\ 1)}\right]}{\left[S^{q_0\ i}\right]}\left[\frac{\left[S^{q_0}\right]}{\left[S^{q_0\ 1}\right]} + 1 + \sum_{j=2}^{i_{max}}\left(\prod_{k=2}^{j}\frac{\left[S^{q_0\ k}\right]}{\left[S^{q_0\ (k\ 1)}\right]}\right)\right] \quad (14)$$

where $x_{S^{q_0\ (i\ 1)}}$ is the fraction of molecules of species S with an electrical charge of $q_0\ \ (i\ \ 1)$ e and i_{max} is the maximum number of protons the species can donate.

2.4.2. Stability study of UV–Vis absorbance with time

The next step was to assess the stability over time of the UV–Vis absorbance spectrum at different pH values. This was conducted for solutions of the pharmaceutical at pH values near integer values of the mean charge $\overline{q}$ or near the known pH values of the selected ATPS. The former allows to determine the UV-Vis absorbance spectrum of each differently charged antioxidant species, whereas the latter allows to analyze a distribution of antioxidant species similar to the future extractive conditions.

For this, an aqueous stock solution was prepared at the maximum measurable concentration (*i.e.,* the maximum concentration at which the UV–Vis spectrophotometer did not saturate). In this case, a concentration of 1 5·10 ^{4} g·mL ^{1} for acetaminophen was chosen, whereas 1 8·10 ^{3} g·mL ^{1} were selected for both amoxicillin and salicylic acid. Then, the pH was adjusted using either a 0.5 M aqueous solution of acetic acid or sodium hydroxide, and the ultraviolet-visible (UV-Vis) absorbance spectra were determined at 298.15 K, both at the day the solutions were prepared and 3 days after, to verify whether the absorbance spectrum and intensity were maintained.

2.4.3. UV–Vis absorbance calibration curve

For each of the studied pharmaceuticals, a UV–Vis absorbance calibration curve was determined at the system's pH at its optimal concentration: either at the solute's solubility in water or at the maximum measurable concentration.

For this, a stock solution of each solute was adjusted to the ATPS's pH and left to settle for roughly 24 h. Solutions of known concentrations were prepared by diluting the stock solution to a total volume of 2 mL. The vials were capped, sealed, and stirred, and an UV–Vis absorbance scanning, from 200 to 600 nm, was carried out by pipetting 200 L into a 96-well polystyrene flat bottom plate. After subtracting the water and plate absorbance, a first-degree fitting of the resulting absorbance at the wavelength of a local maximum of the UV–Vis spectrum (λ_{max}) was performed.

2.4.4. Determination of the blanks of the ATPSs and partitions

The blanks of the ATPS must be determined before performing the solute partitioning, so 10 g of initial mixture were prepared in vials, according to the known tie-lines, by pipetting and measuring the mass of the compounds. Then, vials were capped and sealed to avoid mass losses by evaporation. The initial ternary mixtures were stirred using a VWR VV3 vortex for 1 min and in an IKA RO 10 P magnetic stirrer for 6 h at 298.15 K, then settled overnight (around 12 h) at the same temperature, allowing to reach equilibrium. Then, phases were separated using an Eppendorf Multipipette E3x, and mass, UV-Vis absorbance spectra from 200 to 600 nm, pH and liquid density of each phase were measured.

The partition of the solute was carried out analogously to the preparation of the ATPS blanks, the difference being that 1 mL of the water content was replaced with the solute's stock solution. The remaining procedure was carried out identically to the one described above.

Then, an analysis of the results was performed so as to quantify the carried-out extractions. Mass losses (L_m) in phase separation were calculated as:

$$L_m = \frac{m^T + m^B\ \ m^M}{m^M}\cdot 100\% \quad (15)$$

where m^M, m^T and m^B are the masses of initial mixture, top phase, and bottom phase, respectively. Mass losses allow to quantify the mass losses in the physical separation of the two phases.

The UV–Vis absorbance of the corresponding blank was subtracted from the one of each phase, allowing to determine the solute concentration of each phase using the calibration curve. Next, the partition coefficients (K) were calculated as the ratio between the solute concentration (in g/mL) the in top and bottom phases (C_i^T and C_i^B, respectively), as Eq. (16) shows.

$$K_i = \frac{C_i^T}{C_i^B} \quad (16)$$

The volume of each phase was calculated by dividing the phase mass by the respective liquid density and, subsequently, were employed in the calculation of the solute losses ($L_{s,i}$, Eq. (17)):

$$L_{s,i} = \frac{C_i^T V_i^T + C_i^B V_i^B\ \ m_i^{s,M}}{m_i^{s,M}}\cdot 100\% \quad (17)$$

where V_i is the volume of phase and $m_i^{s,M}$ is the mass of solute present in 1 mL of added stock solution. T and B refer to the top and bottom phases, respectively. As opposed to the mass losses (L_m), the solute losses refer to the losses during quantification and translate a deviation from the mass balance of the system.

The extraction efficiency (E), a useful indicator of each tie-line's performance, can also be calculated from the phase concentrations and volumes, as shown in Eq. (18).

$$E_i = \frac{C_i^T V_i^T}{m_i^{s,M}}\cdot 100\% \quad (18)$$

Extraction efficiencies allow to quantify the mass percentage of each solute recovered in the top phase of each tie-line. Nonetheless, as the solute losses calculated by Eq. (17) could be in the top phase, a maximum value of the extraction efficiency can be estimated by adding the solute losses L_s to the calculated extraction efficiency E, whereas E is the lower bound of this interval. The maximum value of E can be calculated according to Eq. (19):

$$E_{i,max}\ \ = E_i + L_{s,i} \quad (19)$$

3. Experimental results and discussion

3.1. Liquid-liquid equilibria (LLE) data

3.1.1. Demixing tests and solubility curves

In this work, 11 systems were tested regarding their immiscibility. Table 2 presents the tested ranges of compositions for each system, and the obtained number of points. It is worth noting that, for systems where immiscibility was observed, the range of tested compositions was limited by the concentrations of the saturated salt or polymer solutions employed (namely mass fractions of $w_{PEG1500} = 0\ 66$, $w_{PEG4000} = 0\ 50$, $w_{PVP29000} = 0\ 39$ for the polymers, and $w_{[Ch][Bic]} = 0\ 80$, $w_{[Ch][Bit]} = 0\ 62$, $w_{[Ch]Cl} = 0\ 36$ and $w_{[Ch][DHCit]} = 0\ 78$ for the choline salts). On the other hand, if demixing was not observed in a large range of composition, the remaining concentrations were not tested, as the system would likely not produce sufficiently long tie-lines, which would not be promising for liquid-liquid extraction.

The LLE data for the system {PEG4000 (1) + [Ch][DHCit] (2) + water (3)} has been reported by Mourão, et al. [34]. In parallel to this work, Souza, et al. [35] studied ternary systems containing polyethylene of average molecular masses 400 and 1500 g·mol ^{1} and choline salts, namely [Ch]Cl, [Ch][Bit] and [Ch][DHCit] and presented the binodal curve of these ATPSs (which can be obtained by joining tie-line compositions, thus differing from solubility curves). Finally, as best of the authors' knowledge, there are no reports of other EL-based systems containing choline salts, so these systems were studied first-hand in this work. The experimental mass fractions of the points in the solubility curves can be found in the Supplementary Materials (Table S1).

Table 2
List of the tested systems and respective range of compositions.

System	Number of points	Range of tested compositions		Demixing verified?[a]
		w_1	w_2	
{EL (1) [Ch] Cl (2) water (3)}	0	0.00 – 1.00	0.00 – 0.32	no
{EL (1) [Ch] [Bit] (2) water (3)}	22	0.00 – 1.00	0.00 – 0.57	yes
{EL (1) [Ch] [DHCit] (2) water (3)}	9	0.00 – 1.00	0.00 – 0.71	yes
{EL (1) [Ch] [Bic] (2) water (3)}	5	0.00 – 1.00	0.00 – 0.80	yes
{PEG1500 (1) [Ch] [DHCit] (2) water (3)}	6	0.00 – 0.55	0.00 – 0.78	yes
{PEG1500 (1) [Ch] [Bit] (2) water (3)}	5	0.00 – 0.66	0.00 – 0.45	yes
{PEG4000 (1) [Ch] Cl (2) water (3)}	0	0.05 – 0.25	0.26 – 0.36	no
{PEG4000 (1) [Ch] [Bit] (2) water (3)}	13	0.00 – 0.48	0.00 – 0.60	yes
{PVP29000 (1) [Ch] Cl (2) water (3)}	0	0.02 – 0.12	0.00 – 0.30	no
{PVP29000 (1) [Ch] [Bit] (2) water (3)}	0	0.09 – 0.39	0.00 – 0.48	no
{PVP29000 (1) [Ch] [DHCit] (2) water (3)}	0	0.09 – 0.39	0.00 – 0.62	no

[a] 'yes' indicates that demixing occurred and that a biphasic mixture was obtained, while 'no' means that the components were miscible in the tested range of compositions.

Furthermore, the data of the solubility curves were then fitted to the Merchuk [37], Li [38], and Yu [39] correlations (Eqs. (1) to (3)), by minimization of the Root Mean Squared Error. For each system, the optimized parameters are shown in Table 3.

Table 3
Parameters of the Merchuk [37], Li [38], and Yu [39] correlations, for the new ternary systems, at 298.15 K and 0.1 MPa.

	Parameters				Performance Indicators	
{EL (1) [Ch] [Bit] (2) Water (3)}						
Model	A_1	B_1	C_1	D_1	R^2	E_{RMSE} /%
Merchuk	1.074	1.612	9.917	–	0.9926	2.22
Li	0.973	0.491	1.737	0.850	0.9996	0.524
Yu	0.0299	1.279	0.01389	370.9	0.9984	1.02
{EL (1) [Ch] [Bic] (2) Water (3)}						
Model	A_1	B_1	C_1	D_1	R^2	E_{RMSE} /%
Merchuk	3.458	4.362	1.128	–	0.9944	1.13
Li	1.334	1.826	0.3157	3.6056	0.9986	0.572
Yu	1.333	4.642	0.00277	370.8	0.9933	1.23
{EL (1) [Ch] [DHCit] (2) Water (3)}						
Model	A_1	B_1	C_1	D_1	R^2	E_{RMSE} /%
Merchuk	1.313	1.609	3.915	–	0.9994	0.609
Li	1.209	1.310	0.0342	0.1367	0.9988	0.849
Yu	0.0836	0.937	0.00874	370.9	0.9992	0.726
{PEG4000 (1) [Ch] [Bit] (2) Water (3)}						
Model	A_1	B_1	C_1	D_1	R^2	E_{RMSE} /%
Merchuk	0.501	0.463	21.6	–	0.9994	0.233
Li	1.243	2.061	0.0746	10.85	0.9949	0.668
Yu	2.358	4.395	0.0475	370.6	0.9988	0.333
{PEG1500 (1) [Ch] [DHCit] (2) water (3)}						
Model	A_1	B_1	C_1	D_1	R^2	E_{RMSE} /%
Merchuk	0.398	0.399	7.682	–	0.9975	0.793
Li	1.292	1.590	0.0972	3.221	0.99993	0.121
Yu	3.198	5.750	0.0267	370.9	0.9968	0.897
{PEG1500 (1) [Ch] [Bit] (2) water (3)}						
Model	A_1	B_1	C_1	D_1	R^2	E_{RMSE} /%
Merchuk	1.069	2.113	4.368	–	0.9977	0.674
Li	0.220	2.986	6.584	0.683	0.9995	0.301
Yu	2.031	10.25	18.94	0.493	0.9992	0.366

The Merchuk equation presented suitable results for systems containing EL and organic salts [20], but the same was not verified for systems comprising inorganic salts [24]. Nevertheless, for the systems {EL (1) + [Ch][Bit] or [Ch][Bic] (2) + water (3)}, fittings following Li's correlation showed a smaller error and larger R^2, while the model proposed by Merchuk resulted in the best fitting for {EL (1) + [Ch][DHCit] (2) + water (3)}. For the system based on PEG4000 and [Ch][Bit] and for the two ATPSs containing PEG1500, Li's correlation had the best performance.

Fig. 1 presents the solubility curves of the six novel ATPSs. The data were adjusted to the model which produced the best results.

Furthermore, several systems based on PEG with different average molar masses and choline bitartrate were found in literature [32]. A comparison between the new solubility curve for the system {PEG4000 (1) + [Ch][Bit] (2) + water (3)} and the ones previously reported in literature [32], for PEG with average molar masses of 400, 600 and 1000 g·mol ^{1}, can be seen in Fig 2.

Fig. 2 hints that the higher the molar mass of PEG, the closer the solubility curve is to the origin of the phase diagram, which means that lower concentrations of each component are required to attain the immiscible region and form the ATPS. This is due to the fact that PEG polymers with longer alkyl chains are more hydrophobic, therefore more non-polar, resulting in lower solubilities in water and larger immiscible zones. On the other hand, polymers with lower molar masses have shorter alkyl chain lengths and higher solubilities in water.

3.1.2. *Determination of tie-line compositions*

Due to its suitable solubility curve (*i.e.*, the longest), the ATPS {EL (1) + [Ch][Bit] (2) + water (3)} was selected for further studies. So, mixtures were prepared on the homogenous zone (under the solubility curve) to correlate composition with liquid density (ρ) and electrical conductivity ( ), using third-degree polynomials. The measured values of these thermophysical properties can be found in Tables S2 and S3 in the Supplementary Materials, respectively. Table 4 shows the obtained correlations.

The proposed regressions were validated by means of *F*-tests and the results can be found in Table S4, in the Supplementary Materials. In Fig. 3, the plots for the measured thermophysical properties can be observed.

With these correlations, Eqs. (4) to (7) were applied to determine phase equilibrium compositions, yielding the experimental mass fractions, tie-line lengths (TLLs) and slopes (STL) shown in Table 5. The numbering of tie-lines was conducted so as that the shortest tie-line (with the lowest TLL) corresponded to the one with the lowest index.

As Fig. 4 illustrates, the three tie-lines presented similar slope (STL) and were nearly parallel. Moreover, the critical point was determined by calculating the compositions at which the tie-line length was equal to 0. For this, the compositions of the two phases in equilibrium ($w_{1,T}$ and $w_{2,B}$) were extrapolated in each tie-line until a sole point of the solubility curve was obtained, as reported in literature [2]. Compositions of points in the solubility curve were estimated using the best fitting for this ATPS (Li's equation), as previously shown in Table 3. Hence, the composition of the critical point of this ATPS was found to be w_{EL} = 0 3944 and $w_{[Ch]Bit}$ = 0 2443, and the complete ternary diagram can be observed in Fig. 4.

Finally, as it is common in literature, tie-line compositions were fitted to the Othmer-Tobias [41] and Bancroft-Hubard [42] correlations (Eqs. (10) and (11), respectively). The optimized parameters are presented in Table 6.

A satisfactory linearization was obtained in both cases, although the Othmer-Tobias fitting displayed a R^2 closer to unity (0.9689) than Bancroft-Hubard (0.9969).

In summary, the novel ternary system {EL (1) + [Ch][Bit] (2) + water (3)} determined in this work presented three tie-lines, all with a considerable length (> 0.6192). In this system, the top phase is rich in EL

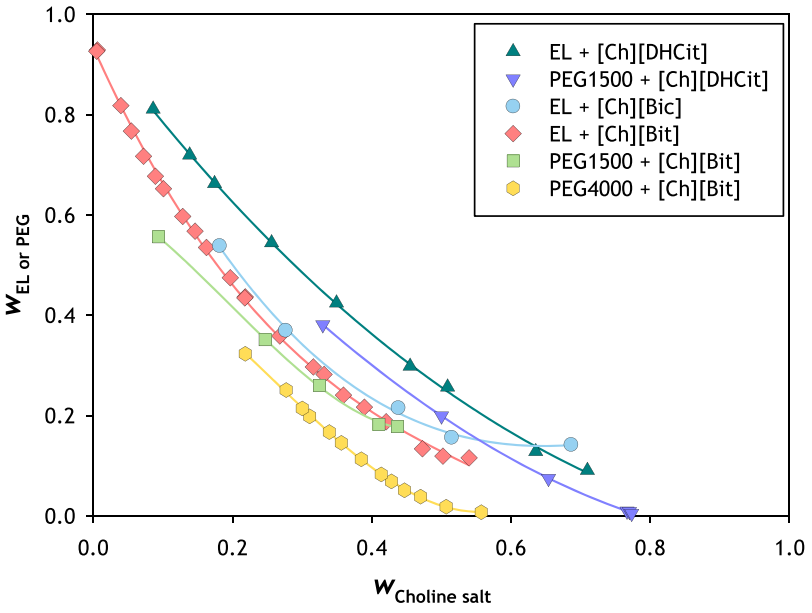

Fig. 1. Experimental solubility curves at 298.15 K and 0.1 MPa. Fittings (–) were carried out following the Merchuk equation (for {EL (1) + [Ch][DHCit] (2) + water (3)}) [37] and the Li equation (for {EL (1) + [Ch][Bit] or [Ch][Bic] (2) + water (3)}, {PEG4000 (1) + [Ch][Bit] (2) + water (3)} and {PEG1500 (1) + [Ch][DHCit] or [Ch][Bit] (2) + water (3)}) [38]. Data are expressed in mass fraction.

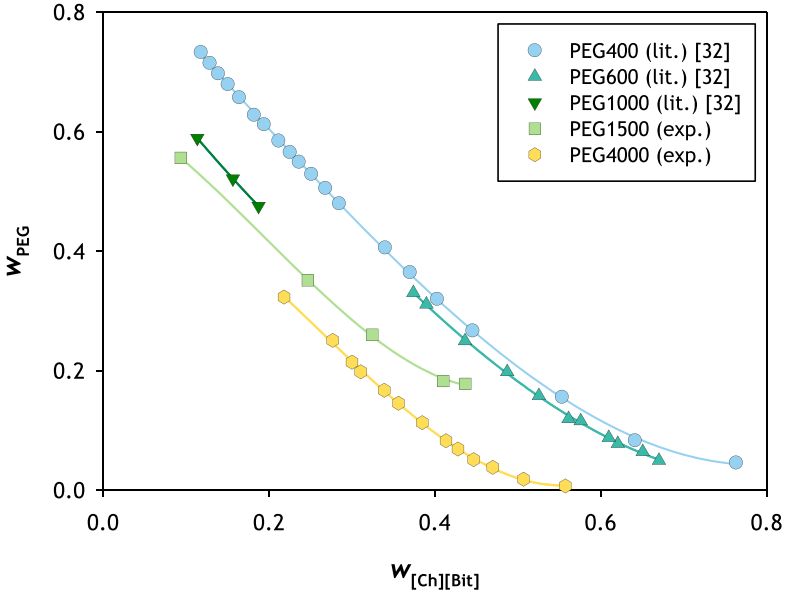

Fig. 2. Comparison between solubility curves of ternary systems containing PEG with different molar masses and choline bitartrate, at 298.15 K and 0.1 MPa: {PEG400 [32] or PEG600 [32] or PEG1000 [32] or PEG1500 (this work) or PEG4000 (this work) (1) + [Ch][Bit] (2) + water (3)}. Data are expressed in mass fraction.

Table 4
Polynomial expressions for liquid density (ρ) and electric conductivity ( ), as function of composition, for the ternary system {EL (1) + [Ch][Bit] (2) + water (3)}, at 298.15 K and 0.1 MPa, and respective relative errors and determination coefficients (R^2).

	Liquid density (ρ, in kg·m ^{3})					Electrical conductivity (, in S·m ^{1})				
	A_1	B_1	C_1	relative error [a]	R^2	A_1	B_1	C_1	relative error	R^2
EL	1071	156.7	122.2	$6.69 \bullet 10^{-4}$	0.9995	9.922	16.38	6.461	0.229	0.9859
Salt	1247	12.04	62.87			9.092	21.06	11.12		
Water	1134	237.8	99.51			3.452	3.037	6.488		

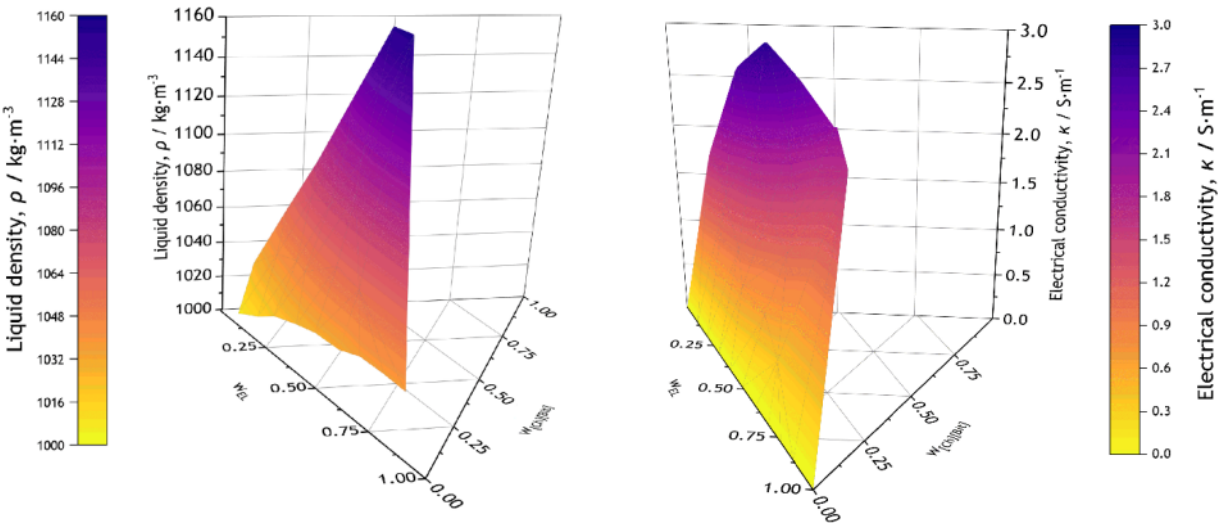

Fig. 3. Three-dimensional ternary plot of liquid density (ρ, left) and electrical conductivity (, right) as a function of the mass fraction of ethyl lactate (EL) and choline (2R,3R)-bitartrate ([Ch][Bit]).

Table 5
Phase equilibrium compositions (mass fractions), tie-line lengths (TLL) and slopes (STL) for the system {EL (1) + [Ch][Bit] (2) + water (3)}, at 298.15 K and 0.1 MPa.

TL	$w_{1,M}$ [a,b]	$w_{2,M}$	$w_{1,T}$	$w_{2,T}$	$w_{1,B}$	$w_{2,B}$	STL	TLL
1	0.2940	0.3536	0.6829	0.0886	0.1788	0.4482	1.40	0.6192
2	0.5039	0.2488	0.7869	0.0494	0.1267	0.5098	1.43	0.8050
3	0.6899	0.1505	0.8391	0.0409	0.1250	0.5578	1.38	0.8816

[a] Indices F, T and B stand for the initial mixture, top and bottom phases, respectively.
[b] The standard measurement uncertainties (u) are: $u(w) = 0\ 0001$, $u(T) = 0\ 01$ K and $u(P) = 2$ kPa.

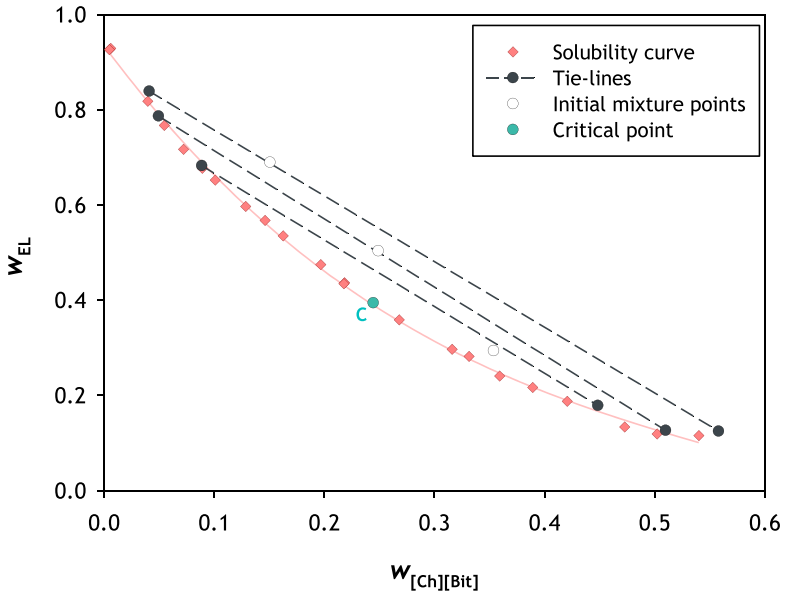

Fig. 4. Solubility curve (fitted by Li's equation [38]) and tie-lines for the novel system {EL (1) + [Ch][Bit] (2) + water (3)}, at 298.15 K and 0.1 MPa. C denotes the critical point, with $w_1 = 0\ 3944$ and $w_2 = 0\ 2443$. Data are expressed in mass fraction.

and water and contains less than 10 % in salt. The solvents used (ethyl lactate and water) can be easily evaporated at reduced pressure, allowing the extracted solute to be obtained in its solid state without the need for high-temperature processing. This could be particularly useful to extract phenolic compounds, such as vitamins or antioxidants, which easily degrade at high temperatures [45]. The solute would be obtained in an extract also containing a small percentage of choline (2R, 3R)-bitartrate – an organic salt, frequently used as a food additive, which is known to possess lipotropic and nootropic properties [36]. Lipotropic properties refer to its ability to increase the transport of lipids in the organism, while nootropic properties denote its ability to facilitate memory and learning and to prevent dementia. Hence, the obtained

Table 6
Parameters obtained using Othmer–Tobias (OT) and Bancroft-Hubard (BH) equations and respective determination coefficients (R^2) for the system {EL (1) + [Ch][Bit] (2) + water (3)}, at 298.15 K and 0.1 MPa.

	Othmer-Tobias			Bancroft-Hubard		
	S_{OT}	n_{OT}	R^2	S_{BH}	n_{BH}	R^2
Parameters	1.1990	2.0183	0.9969	0.3173	0.4421	0.9689

extracts could safely be applied in food supplementation, for example.

3.2. Partitions

Besides their use in biomolecule extraction, another especially important field of application for this ATPS would be the removal of contaminants from polluted water streams [9,10,15,30,31], for which three pharmaceuticals (acetaminophen, amoxicillin and salicylic acid) were selected for partition studies.

3.2.1. Effect of pH on the mean electrical charge

The pK_a values of the three APIs were found in literature: for acetaminophen pK_a = 9 55 [46], for amoxicillin p$K_{a,1}$ = 2 60, p$K_{a,2}$ = 7 31 and p$K_{a,3}$ = 9 53 [47], and for salicylic acid p$K_{a,1}$ = 2 78 and p$K_{a,2}$ = 13 77 [48].

Using these values, equations (29) to (31) were applied, and the mean electrical charges ($\bar{q}$) were obtained as a function of pH for each pharmaceutical, as Fig. 5 shows. Due to the proximity to the first pK_a of salicylic acid and amoxicillin, the mean electrical charge distributions of these two species are similar for pH values below 5. The calculated mean charges and relative abundances of the distinct stages of the amoxicillin and salicylic acid are presented, respectively, in Tables S5 and S6, in the Supplementary Materials. Concerning acetaminophen, these data were obtained from a previous work of the research group [15].

As can be seen in Fig. 5, at the characteristic pH of the ATPS, amoxicillin and salicylic acid are predominantly found at their stage with charge 1 e, while acetaminophen is present in its neutral form (0 e).

3.2.2. Effect of pH on the UV–Vis absorbance spectra

The effect of pH on the UV–Vis absorbance spectra for acetaminophen was carried out in a previous study [15], while, for amoxicillin and salicylic acid, solutions with a known concentration of each pharmaceutical were prepared, and their pH values were adjusted. Then, the UV–Vis absorbance spectra were measured and normalized using a ratio of concentrations. Table 7 shows the stability of the UV–Vis absorbance spectra of acetaminophen, amoxicillin and salicylic acid, while Figs. S1-S9, in the Supplementary Materials, illustrate the UV–Vis spectra of the solutions at the day of preparation and after 3 days.

Given that the studied ternary system exhibited a pH of 3 - 4 and that the UV–Vis spectra were stable within this range, UV–Vis spectroscopy could be used as a quantification method of these APIs.

3.2.3. UV–Vis calibration curves

Since the ATPS {EL (1) + [Ch][Bit] (2) + water (3)} presented pH values close to 4, the calibration curves of the three solutes (acetaminophen, amoxicillin and salicylic acid) were determined at this pH. Following the measurement of UV–Vis absorbance spectra (200–600 nm) of the prepared solutions, maximum wavelengths, corresponding to relative maxima in UV–Vis absorbance, were determined for each API (259 nm for acetaminophen, 272 nm for amoxicillin and 322 nm for salicylic acid). Then, calibration curves were determined at that wavelength, as Fig. 6 shows. The UV–Vis absorbance spectra of aqueous solutions of the pharmaceutical components can be observed in Fig. S10, in the Supplementary Materials, and the concentration and absorbance values used in the calibration curves can be found in Table S7, in the Supplementary Materials.

The obtained UV–Vis calibration curves showed a determination coefficient superior to 0.995 and respected all other validation criteria, for which were considered appropriate. In addition, the limits of detection and quantification were calculated for each curve, which can

Table 7
Stability of the UV–Vis absorbance spectra of acetaminophen [15] (Acet), amoxicillin (Amox) and salicylic acid (SA) after settling for 3 days at 298.15 K and 0.1 MPa.

	pH = 3	pH = 5	pH = 6	pH = 7	pH = 9	pH = 10	pH = 12
Acet [15]	mostly stable	[a]	stable	stable	stable		stable
Amox	stable	stable		stable			stable
SA	mostly stable					stable	stable

[a] This stability was not assessed.

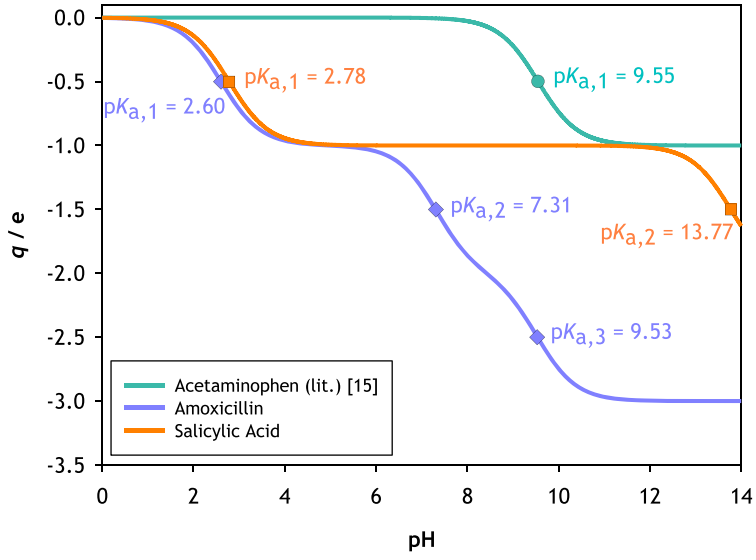

Fig. 5. Calculated mean electrical charge ($\bar{q}$) for acetaminophen [15], amoxicillin and salicylic acid, expressed in terms of the elementary charge (e, *i.e.*, 1 602 · 10 ^{19} C).

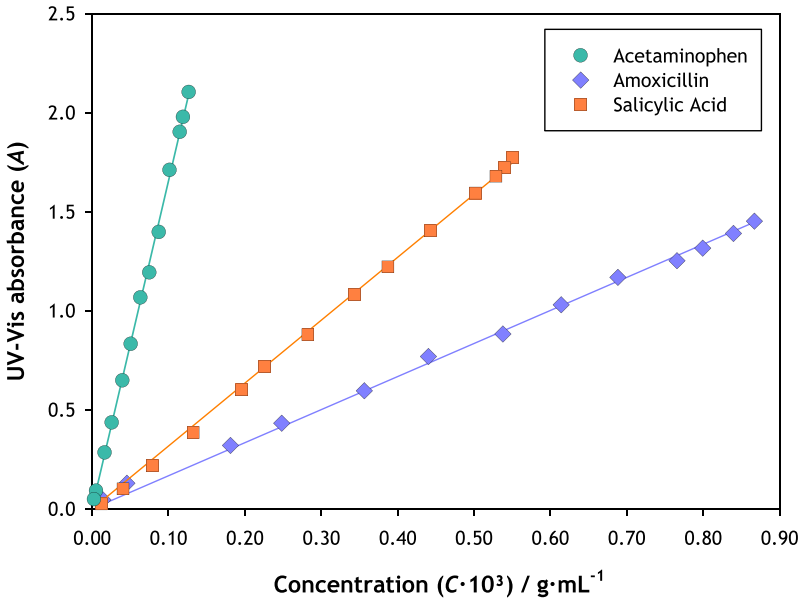

Fig. 6. UV–Vis absorbance calibration curves for acetaminophen (Acet, 259 nm), amoxicillin (Amox, 272 nm) and salicylic acid (SA, 322 nm), at pH = 3. The first-degree fittings are: $A = 16\ 525\ 5 \cdot C_{Acet} + 0\ 00198$ with $R^2 = 0\ 9991$, $A = 1617\ 00 \cdot C_{Amox}$ 0 0347 with $R^2 = 0\ 9989$ and $A = 3244\ 8 \cdot C_{SA} + 0\ 0289$ with $R^2 = 0\ 9988$.

be found in Table S8, in the Supplementary Materials.

Additionally, as can be seen in Fig. S11, in the Supplementary Materials, ethyl lactate, water and choline (2R,3R)-bitartrate do not have a significant UV–Vis absorbance at the wavelengths of the used absorbance maxima, therefore indicating that the chosen wavelength could allow for an accurate quantification of the solutes at this pH using the determined calibration curves.

3.2.4. *Partition coefficients and extraction efficiencies*

Acetaminophen, amoxicillin and salicylic acid were recovered in the novel ATPS determined in this work, following the experimental procedure detailed in Section 2.4.4. The ternary mixtures were prepared following the overall compositions shown in Table 5 ($w_{1,M}$ and $w_{2,M}$), replacing 1 mL of water by 1 mL of aqueous solution of API, with no pH adjustment, meaning that the value of pH presented in Table 8 is the native pH of each mixture. Seeing that the added concentration of API is very low (10^{-4} - 10^{-3} g/mL), it is considered that it does not alter the composition of the phases, which is the same as shown in Table 5 ($w_{1,T}$, $w_{1,B}$, $w_{2,T}$ and $w_{2,B}$).

Then, after stirring and overnight settling, the phases were carefully separated, and their mass (m), UV–Vis absorbance (A), pH, and liquid density (ρ) were measured, for both top and bottom phases, yielding the results presented in Table 8. Moreover, the mass losses during phase separation (L_m), obtained using Eq. (15), and the calculated mass fractions of the target APIs in each phase (w_{API}) are also given in Table 8.

The performance indicators of extraction (partition coefficients (K) and extraction efficiencies (E)) were calculated, as Table 9 shows. It is worth noting that, in the cases where the solute could not be quantified in one of the phases (*i.e.* amoxicillin in the top phases of the tie-lines), the performance indicators were calculated using the limit of quantification of the calibration curve instead of the top phase concentration. Table 9 also shows the solute losses in quantification (L_s), calculated following Eq. (17) and related to quantification errors, as well as the respective tie-line lengths (TLLs).

The partitions of acetaminophen and salicylic acid were performed with mass losses in the phase separation inferior to 5 %. The extraction of amoxicillin presents larger values of L_s, sometimes even positive. This would apparently indicate that an excess of amoxicillin was quantified, regarding what was first introduced in the ATPS. Nonetheless, this can be explained since this API was present in the top phase at a concentration below the limit of quantification of the calibration curve, but K and E were calculated using the quantification limit as the top phase concentration. This was done so that the excess mass artificially introduced in the calculations outweighs the mass losses in phase separation, hence $L_s > 0$. The partition coefficients and extraction efficiencies are plotted as a function of the tie-line length in Fig. 7.

Table 8
Experimental mass of each phase (m), mass losses in phase separation (L_m), solute mass fractions (w_{API}), phase density (ρ) and phase pH for the top and bottom phases in the extraction of acetaminophen, amoxicillin and salicylic acid in the ATPS {EL (1) + [Ch][Bit] (2) + water (3)}, at 298.15 K and 0.1 MPa [a].

Tie-line	Phase	Mass of phase / g	Mass losses, L_m /%	Solute mass fraction, w_{API}	Phase density, ρ / g·cm^{-3}	pH
Acetaminophen						
TL1	top	2.1392	0.6	$8.065 \cdot 10^{-5}$	1.05093	4.68
	bottom	7.8248		$3.296 \cdot 10^{-5}$	1.14934	4.06
TL2	top	5.4209	0.7	$5.709 \cdot 10^{-5}$	1.04972	4.76
	bottom	4.3617		$2.553 \cdot 10^{-5}$	1.16867	3.98
TL3	top	7.8125	1.0	$4.810 \cdot 10^{-5}$	1.04565	4.92
	bottom	2.1214		$2.510 \cdot 10^{-5}$	1.18948	3.81
Amoxicillin						
TL1	top	2.0776	1.0	$< 5.349 \cdot 10^{-5}$ (n.q.) [b]	1.05327	4.37
	bottom	7.8334		$1.326 \cdot 10^{-4}$	1.14821	3.93
TL2	top	5.5814	1.0	$< 5.349 \cdot 10^{-5}$ (n.q.)	1.04842	4.59
	bottom	4.2201		$2.312 \cdot 10^{-4}$	1.16394	3.98
TL3	top	7.8186	0.9	$< 5.349 \cdot 10^{-5}$ (n.q.)	1.04347	4.81
	bottom	2.1025		$4.205 \cdot 10^{-4}$	1.18177	4.65
Salicylic acid						
TL1	top	2.0441	1.0	$3.738 \cdot 10^{-4}$	1.05367	4.46
	bottom	7.9252		$5.948 \cdot 10^{-5}$	1.14836	4.33
TL2	top	5.4863	0.9	$1.957 \cdot 10^{-4}$	1.04831	4.62
	bottom	4.4861		$2.763 \cdot 10^{-5}$	1.16745	4.19
TL3	top	7.7359	0.4	$1.536 \cdot 10^{-4}$	1.04473	4.74
	bottom	2.2264		$1.519 \cdot 10^{-5}$	1.18352	4.24

[a] The standard measurement uncertainties (u) are: $u(m) = 10^{-4}$ g, $u(\rho) = 10^{-5}$ g·cm^{-3}, $u(\text{pH}) = 0\ 01$, $u(T) = 0\ 01$ K and $u(P) = 2$ kPa.
[b] (n.q.) stands for not quantified.

Table 9
Calculated solute losses (L_s), extraction efficiency (E) intervals, partition coefficients (K) and values of tie-line lengths (TLL) for the partitions of acetaminophen, amoxicillin and salicylic acid in the ATPS {EL (1) + [Ch][Bit] (2) + water (3)}, at 298.15 K and 0.1 MPa.

Tie-line	Solute losses, L_s /%	Partition coefficient, K	Extraction efficiencies, E /%	Tie-line length, TLL
Acetaminophen				
TL1	2.8	2.2 ± 0.1	(39.1 41.7) ± 0.1	0.6192
TL2	4.9	2.0 ± 0.1	(70.0 74.8) ± 0.2	0.8050
TL3	3.6	1.7 ± 0.1	(84.5 88.0) ± 0.2	0.8816
Amoxicillin				
TL1	9.1	< 0.37 ± 0.09	< 9.60 ± 0.02	0.6192
TL2	9.8	< 0.21 ± 0.05	< 25.81 ± 0.03	0.8050
TL3	0.68	< 0.11 ± 0.03	< 35.27 ± 0.04	0.8816
Salicylic acid				
TL1	2.9	5.6 ± 0.3	(59.42 62.33) ± 0.07	0.6192
TL2	3.9	6.4 ± 0.7	(86.13 90.06) ± 0.09	0.8050
TL3	2.2	9 ± 2	(95.1 97.3) ± 0.1	0.8816

As illustrated by Fig 7, this novel ATPS is more selective towards the extraction of salicylic acid and acetaminophen than towards amoxicillin, as these partitions produced partition coefficients above unity (or ln$K$ > 0). In fact, values of the partition coefficient inferior to unity were obtained for amoxicillin, showing that the top phase had a lower concentration of amoxicillin than the top phase. For acetaminophen and salicylic acid, larger values of K were obtained. Furthermore, their extraction efficiencies were higher for the longest tie-line, hinting at a more favorable extraction with larger content of ethyl lactate.

Moreover, the partition coefficients and extraction efficiencies of acetaminophen were compared to ones obtained in a previous study [15], in which acetaminophen was partitioned in five CAAIL-based ATPSs at 298.15 K and 0.1 MPa. Four of these ATPSs {[Ch][Ala] or [Ch][Gly] (1) + K_2HPO_4 (2) + water (3)} and {[Ch][Ala] or [Ch][Leu] (1) + K_3PO_4 (2) + water (3)}) showed promising results for the extraction of acetaminophen, allowing to obtain extraction efficiencies of > 97 % for the longest tie-lines, which are higher than the values obtained using this ATPS. Partition coefficients were also higher than the ones found in this work. Nonetheless, using an EL-based ATPS provides an easy recovery of the extracted solute by evaporation of the solvents, and allows the further application of the extracts. On the other hand, the synthesis of ionic liquid is avoided, averting a consumption of organic solvents (such as ethanol) [15]. On the particular case of CAAILs, as these solvents lack scientific maturity, a complete assessment of their toxicity according to criteria defined in the Registration, Evaluation, Authorisation and Restriction of CHemicals (REACH) regulation is also needed [49].

Using the measured pH values, the relative abundances of each of the various forms of the pharmaceuticals in solution were assessed, thus verifying the effect of tie-line composition in the distribution of the differently charged stages. The obtained results can be observed in Fig. 8, which shows, once again, that the studied ATPS allowed to extract mostly the neutral stage of acetaminophen (q = 0 e) and the negatively charged stages of amoxicillin and salicylic acid (q = 1 e). However, no relation was found between stage distribution and solute migration, which may be explained by attenuation in dipolar moments due to changes in chemical conformation.

Fig. 8 shows that the tie-lines of the novel system {EL (1) + [Ch][Bit] (2) + water (3)} only allowed to extract the neutral form of acetaminophen, given that the pH of the phases was lower than its pK_a (9.55). Amoxicillin and salicylic acid are predominantly found at their stage with charge 1 e, as the pH of the phases was between their values of p$K_{a,1}$ and p$K_{a,2}$. Since there was no significant variation (< 5 %) in the stages present in different tie-lines, the application of the same calibration curve for both top and bottom phases of this ATPS was validated.

4. Conclusions

In this work, demixing tests were conducted for 11 aqueous ternary systems containing choline salts (choline chloride, choline bicarbonate, choline (2R,3R)-bitartrate and choline di-hydrogen citrate) and either ethyl lactate, polyethylene glycol or polyvinylpyrrolidone for application in ATPSs, at 298.15 K and 0.1 MPa. For 6 of these systems, the solubility curves were obtained and fitted to common correlations used in literature.

Due to having the longest solubility curve, the system {ethyl lactate (1) + choline (2R,3R)-bitartrate (2) + water (3)} was selected for further studies, and a total of 3 nearly parallel tie-lines were determined by measurements of thermophysical properties (electrical conductivity and liquid density). Then, tie-line composition data were fitted with Othmer-Tobias and Bancroft-Hubard equations, attaining high determination coefficients.

Finally, the potential of this novel ATPS in the removal of three APIs from aqueous samples was assessed. Salicylic acid was successfully extracted to the top phase, with the highest partition coefficients (K) being obtained for the longest tie-line, which had a length of 0.8816 (K = 9 ± 2 and E ≥ 95 %). On the other hand, acetaminophen was

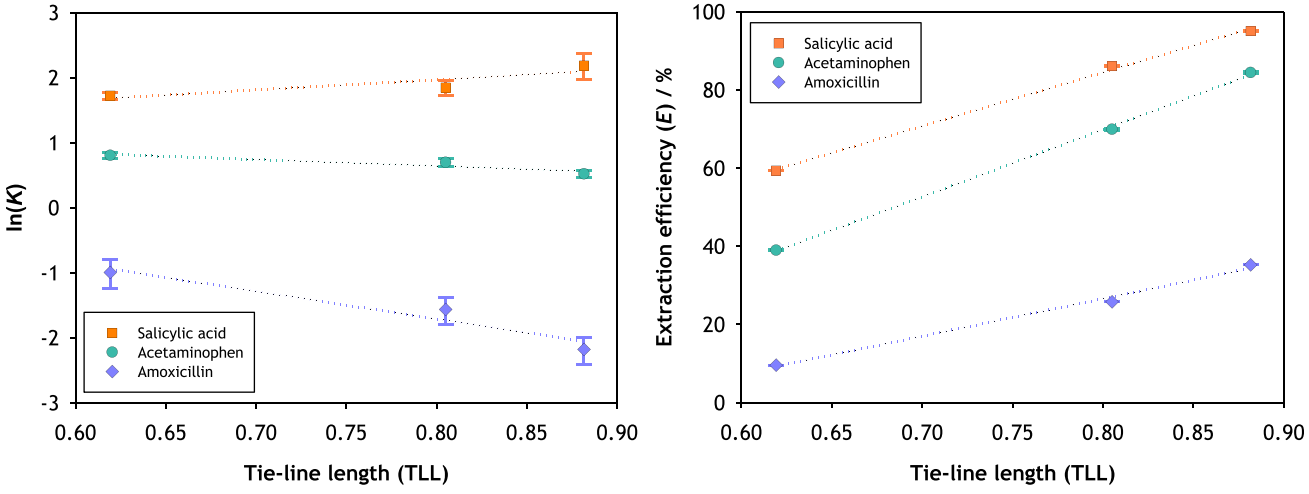

Fig. 7. Relation of the tie-line length (TLL) with the natural logarithm of the experimental partition coefficients (ln$K$, left) and with the extraction efficiency (E, right) for acetaminophen, amoxicillin and salicylic acid, and respective linear regressions in the ATPS {EL (1) + [Ch][Bit] (2) + water (3)}, at 298.15 K and 0.1 MPa.

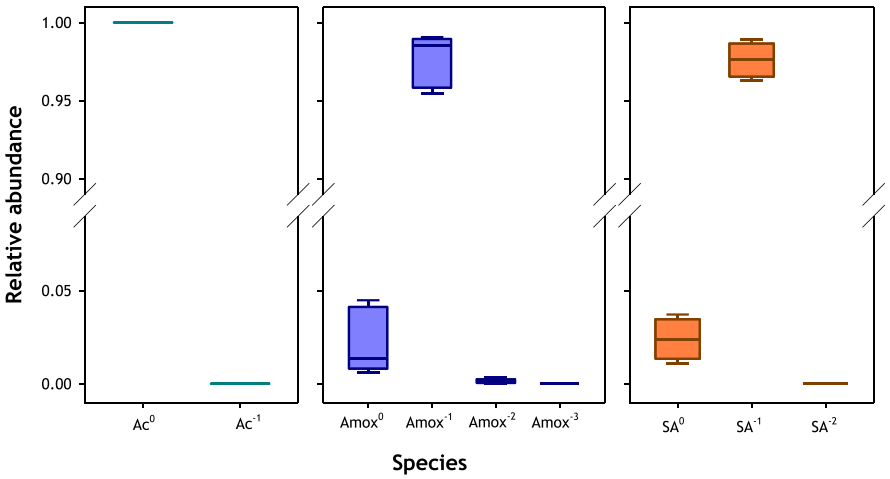

Fig. 8. Influence of the tie-line compositions in the relative abundance (fraction) of the stages of the studied pharmaceuticals in the ATPS {EL (1) + [Ch][Bit] (2) + water (3)}, at 298.15 K and 0.1 MPa. Ac^0 and Ac^{-1} stand for the stages of acetaminophen with electrical charges equal to 0 and 1 e, respectively. $Amox^0$, $Amox^{-1}$, $Amox^{-2}$ and $Amox^{-3}$ stand for the stages of amoxicillin with electrical charges equal to 0, - 1, 2 and 3 e, respectively. SA^0, SA^{-1} and SA^{-2} stand for the stages of salicylic acid with electrical charges equal to 0, - 1 and 2 e. e stands for the elementary charge (1 602·10 ^{19} C).

best extracted with the shortest tie-line, which had a length of 0.6192 ($K = 2\,2 \pm 0\,1$) and amoxicillin showed no affinity for the ethyl lactate-rich phase ($K \leq 0\,11$ and $E < 35\%$).

Due to the biocompatible properties of the components of the novel ATPS, further applications of this system are envisaged, namely in the extraction of bioactive compounds from bio-residues, leading to added-value products.

CRediT authorship contribution statement

Leonor R. Barroca: Writing – review & editing, Writing – original draft, Visualization, Investigation, Formal analysis. **Pedro Velho:** Writing – review & editing, Supervision, Methodology, Investigation, Formal analysis, Conceptualization. **Eugenia A. Macedo:** Writing – review & editing, Supervision, Conceptualization.

Declaration of competing interest

The authors declare that they have no known competing financial interests or personal relationships that could have appeared to influence the work reported in this paper.

Data availability

Data will be made available on request.

Acknowledgements

This work was supported by national funds through FCT/MCTES (PIDDAC): LSRE-LCM, UIDB/50020/2020 (DOI: 10.54499/UIDB/50020/2020) and UIDP/50020/2020 (DOI: 10.54499/UIDP/50020/2020); and ALiCE, LA/P/0045/2020 (DOI: 10.54499/LA/P/0045/2020). Pedro Velho thanks funding support from FCT [2021.06626.BD].

Supplementary materials

Supplementary material associated with this article can be found, in the online version, at doi:10.1016/j.fluid.2024.114193.

References

[1] G. Crini, E. Lichtfouse, Advantages and disadvantages of techniques used for wastewater treatment, Environ. Chem. Lett. 17 (2019) 145–155.
[2] M.G. Freire, A.F.M. Claudio, J.M.M. Araújo, J.A.P. Coutinho, I.M. Marrucho, J.N. C. Lopes, L.P.N. Rebelo, Aqueous biphasic systems: a boost brought about by using ionic liquids, Chem. Soc. Rev. 41 (2012) 4966–4995.
[3] X. Lu, Z. Lu, R. Zhang, L. Zhao, H. Xie, Distribution of pigments in the aqueous two-phase system formed with piperazinium-based ionic liquid and anionic surfactant, J. Mol. Liq. 330 (2021) 115677.
[4] A.M. Ferreira, J.A.P. Coutinho, A.M. Fernandes, M.G. Freire, Complete removal of textile dyes from aqueous media using ionic-liquid-based aqueous two-phase systems, Sep. Purif. Technol. 128 (2014) 58–66.
[5] P.A. Korchak, E.A. Safonova, A.I. Victorov, Amino acid ionic liquids as components of aqueous biphasic systems for L-tryptophan extraction: experiment and thermodynamic modeling with ePC-SAFT equation of state, J. Mol. Liq. 366 (2022) 120185.
[6] P.F. Requejo, P. Velho, E. Gomez, E.A. Macedo, Study of Liquid–Liquid Equilibrium of Aqueous Two-Phase Systems Based on Ethyl Lactate and Partitioning of Rutin and Quercetin, Ind. Eng. Chem. Res. 59 (2020) 21196–21204.
[7] P. Velho, C.S. Rebelo, E.A. Macedo, Extraction of Gallic Acid and Ferulic Acid for Application in Hair Supplements, Molecules 28 (2023) 2369.
[8] P.G. Mazzola, A.M. Lopes, F.A. Hasmann, A.F. Jozala, T.C.V. Penna, P. O. Magalhães, C.O. Rangel-Yagui, A. Pessoa, Liquid–liquid extraction of biomolecules: an overview and update of the main techniques, J. Chem. Technol. Biotechnol. 83 (2008) 143–157.
[9] M.E. Zakrzewska, A.V.M. Nunes, A.R. Barot, A. Fernandez-Castane, Z.P. Visak, W. Kiatkittipong, V. Najdanovic-Visak, Extraction of antibiotics using aqueous two-phase systems based on ethyl lactate and thiosulphate salts, Fluid Ph. Equilib. 539 (2021) 113022.
[10] J.F.B. Pereira, F. Vicente, V.C. Santos-Ebinuma, J.M. Araújo, A. Pessoa, M. G. Freire, J.A.P. Coutinho, Extraction of tetracycline from fermentation broth using aqueous two-phase systems composed of polyethylene glycol and cholinium-based salts, Process Biochem 48 (2013) 716–722.
[11] H.F.D. Almeida, I.M. Marrucho, M.G. Freire, Removal of Nonsteroidal Anti-Inflammatory Drugs from Aqueous Environments with Reusable Ionic-Liquid-Based Systems, ACS. Sustain. Chem. Eng. 5 (2017) 2428–2436.
[12] F.A. Silva, T. Sintra, S.P.M. Ventura, J.A.P. Coutinho, Recovery of paracetamol from pharmaceutical wastes, Sep. Purif. Technol. 122 (2014) 315–322.
[13] H.F.D. Almeida, M.G. Freire, I.M. Marrucho, Improved extraction of fluoroquinolones with recyclable ionic-liquid-based aqueous biphasic systems, Green Chem 18 (2016) 2717–2725.
[14] J.F.B. Pereira, M.G. Freire, J.A.P. Coutinho, Aqueous two-phase systems: towards novel and more disruptive applications, Fluid Ph. Equilib. 505 (2020) 112341.
[15] L.R. Barroca, P. Velho, E.A. Macedo, Removal of acetaminophen (paracetamol) from water using Aqueous Two-Phase Systems (ATPSs) composed of Choline-Amino Acid Ionic Liquids, J. Chem. Eng. Data 69 (2024) 215–226.
[16] S. Al-Saidi, F.S. Mjalli, M. Al-Azzawi, B. Abutarboosh, M.A. AlSaadi, T. Al-Wahaibi, Amoxicillin removal from medical wastewater using an eco-friendly aqueous two-phase extraction system, Sep. Sci. Technol. 58 (2023) 61–74.
[17] K. Wysoczanska, E.A. Macedo, Effect of molecular weight of polyethylene glycol on the partitioning of DNP-amino acids: PEG (4000, 6000) with sodium citrate at 298.15 K, Fluid Ph. Equilib. 428 (2016) 84–91.
[18] E. Gomez, P.F. Requejo, E. Tojo, E.A. Macedo, Recovery of flavonoids using novel biodegradable choline amino acids ionic liquids based ATPS, Fluid Ph. Equilib. 493 (2019) 1–9.

[19] A. Foulet, O.B. Ghanem, M. El-Harbawi, J.-M. Levêque, M.I.A. Mutalib, C.-Y. Yin, Understanding the physical properties, toxicities and anti-microbial activities of choline-amino acid-based salts: low-toxic variants of ionic liquids, J. Mol. Liq. 221 (2016) 133–138.
[20] P. Velho, P.F. Requejo, E. Gomez, E.A. Macedo, Novel ethyl lactate based ATPS for the purification of rutin and quercetin, Sep. Purif. Technol. 252 (2020) 117447.
[21] P. Velho, I. Oliveira, E. Gomez, E.A. Macedo, pH Study and Partition of Riboflavin in an Ethyl Lactate-Based Aqueous Two-Phase System with Sodium Citrate, J. Chem. Eng. Data 67 (2022) 1985–1993.
[22] E. Gomez, E.A. Macedo, Partitioning of DNP-amino acids in ionic liquid/citrate salt based Aqueous Two-Phase System, Fluid Ph. Equilib. 484 (2019) 82–87.
[23] P. Velho, L. Marques, E.A. Macedo, Extraction of Polyphenols and Vitamins Using Biodegradable ATPS Based on Ethyl Lactate, Molecules 27 (2022) 7838.
[24] P. Velho, P.F. Requejo, E. Gomez, E.A. Macedo, Thermodynamic study of ATPS involving ethyl lactate and different inorganic salts, Sep. Purif. Technol. 275 (2021) 119155.
[25] C.S.M. Pereira, V.M.T.M. Silva, A.E. Rodrigues, Ethyl lactate as a solvent: properties, applications and production processes – a review, Green Chem 13 (2011) 2658–2671.
[26] I. Kamalanathan, Z. Petrovski, L.C. Branco, V. Najdanovic-Visak, Novel aqueous biphasic system based on ethyl lactate for sustainable separations: phase splitting mechanism, J. Mol. Liq. 262 (2018) 37–45.
[27] P. Velho, E.A. Macedo, Liquid–Liquid Extraction of Some Biomolecules in the ATPS {Ethyl Lactate (1) + Sodium Potassium Tartrate (2) + Water (3)} at 298.15 K and 0.1 MPa, J. Chem. Eng. Data 68 (2023) 2385–2397.
[28] C.S. Rebelo, P. Velho, E.A. Macedo, Partition Studies of Resveratrol in Low-Impact ATPS for Food Supplementation, Ind. Eng. Chem. Res. (2023).
[29] C.S. Rebelo, P. Velho, E.A. Macedo, eNRTL Modelling and Partition of Phenolics in the ATPSs {Ethyl lactate (1) + Potassium Sodium Tartrate or Disodium Succinate (2) + Water (3)} at 298.2 K and 0.1 MPa, Fluid Ph. Equilib. (2024) 114087.
[30] P. Velho, E. Sousa, E.A. Macedo, Extraction of Salicylic Acid Using Sustainable ATPSs and Respective Immobilization as API-IL at Small Pilot Scale, J. Chem. Eng. Data (2024).
[31] I. Kamalanathan, L. Canal, J. Hegarty, V. Najdanovic-Visak, Partitioning of amino acids in the novel biphasic systems based on environmentally friendly ethyl lactate, Fluid Ph. Equilib. 462 (2018) 6–13.
[32] J.F.B. Pereira, K.A. Kurnia, O.A. Cojocaru, G. Gurau, L.P.N. Rebelo, R.D. Rogers, M. G. Freire, J.A.P. Coutinho, Molecular interactions in aqueous biphasic systems composed of polyethylene glycol and crystalline *vs.* liquid cholinium-based salts, Phys. Chem. Chem. Phys. 16 (2014) 5723–5731.
[33] J.F.B. Pereira, A. Magri, M.V. Quental, M. Gonzalez-Miquel, M.G. Freire, J.A. P. Coutinho, Alkaloids as Alternative Probes To Characterize the Relative Hydrophobicity of Aqueous Biphasic Systems, ACS. Sustain. Chem. Eng. 4 (2016) 1512–1520.
[34] T. Mourão, L.C. Tome, C. Florindo, L.P.N. Rebelo, I.M. Marrucho, Understanding the Role of Cholinium Carboxylate Ionic Liquids in PEG-Based Aqueous Biphasic Systems, ACS. Sustain. Chem. Eng. 2 (2014) 2426–2434.
[35] E.R. Souza, K.d.C. Silva, L.D. Souza, A.B. Mageste, G.D. Rodrigues, L.R. Lemos, Equilibrium phase behavior of ternary systems formed by polyethylene glycol + choline salts + water, Fluid Ph. Equilib. 573 (2023) 113858.
[36] J.K. Blusztajn, Choline, a Vital Amine, Science 281 (1998) 794–795.
[37] J.C. Merchuk, B.A. Andrews, J.A. Asenjo, Aqueous two-phase systems for protein separation: studies on phase inversion, J. Chromatogr. B Biomed. Appl. 711 (1998) 285–293.
[38] Z. Li, Y. Pei, L. Liu, J. Wang, (Liquid+liquid) equilibria for (acetate-based ionic liquids+inorganic salts) aqueous two-phase systems, J. Chem. Thermodyn. 42 (2010) 932–937.
[39] C. Yu, J. Han, S. Hu, Y. Yan, Y. Li, Phase Diagrams for Aqueous Two-Phase Systems Containing the 1-Ethyl-3-methylimidazolium Tetrafluoroborate/1-Propyl-3-methylimidazolium Tetrafluoroborate and Trisodium Phosphate/Sodium Sulfite/Sodium Dihydrogen Phosphate at 298.15 K: experiment and Correlation, J. Chem. Eng. Data 56 (2011) 3577–3584.
[40] P. Velho, E. Gomez, E.A. Macedo, Calculating the closest approach parameter for ethyl lactate-based ATPS, Fluid Ph. Equilib. 556 (2022) 113389.
[41] D.F. Othmer, P.E. Tobias, Liquid-Liquid Extraction Data - Toluene and Acetaldehyde Systems, Ind. Eng. Chem. 34 (1942) 690–692.
[42] W.D. Bancroft, S.S. Hubard, A New Method for Determining Dineric Distribution1, J. Am. Chem. Soc. 64 (1942) 347–353.
[43] A. Arce, A. Arce Jr., O. Rodriguez, Revising Concepts on Liquid–Liquid Extraction: data Treatment and Data Reliability, J. Chem. Eng. Data 67 (2022) 286–296.
[44] P. Velho, L.R. Barroca, E.A. Macedo, Partition of antioxidants available in biowaste using a green aqueous biphasic system, Sep. Purif. Technol. 307 (2023) 122707.
[45] J.K.U. Ling, J.H. Sam, J. Jeevanandam, Y.S. Chan, J. Nandong, Thermal Degradation of Antioxidant Compounds: effects of Parameters, Thermal Degradation Kinetics, and Formulation Strategies, Food Bioprocess Technol 15 (2022) 1919–1935.
[46] I. Dobaš, V. Štěrba, M. Večeřa, Kinetics and mechanism of diazo coupling. X The coupling kinetics of para-substituted phenol, Collect. Czechoslov. Chem. Commun. 34 (1969) 3746–3754.
[47] R.J. Prankerd, Profiles of Drug Substances, Excipients and Related Methodology: Critical Compilation of Pka Values for Pharmaceutical Substances, Elsevier Science, 2007.
[48] K. Takacs-Novak, K.J. Box, A. Avdeef, Potentiometric pKa determination of water-insoluble compounds: validation study in methanol/water mixtures, Int. J. Pharm. 151 (1997) 235–248.
[49] T.P.T. Pham, C.-W. Cho, Y.-S. Yun, Environmental fate and toxicity of ionic liquids: a review, Water Res 44 (2010) 352–372.